Songklanakarin J. Sci. Technol.
43 (6), 1751-1755, Nov. - Dec. 2021

http://www.sjst.psu.ac.th

*Original Article*

# Preparation and characterization of mixed rare earth hydroxide by co- precipitation method♣

Wilasinee Kingkam[1], Sathita Ratnon[2], Saranphon Boonruang[2], Winyu Chitsamphandhvej[2], Vichai Puripunyavanich[1], Sasikarn Nuchdang[1], and Dussadee Rattanapha[1*]

[1] *Nuclear Technology Research and Development Center, Thailand Institute of Nuclear Technology (Public Organization), Ongkharak, Nakhon Nayok, 26120 Thailand*

[2] *Department of Chemistry, Faculty of Science, King Mongkut's University of Technology Thonburi, Thung Khru, Bangkok, 10140 Thailand*

Received: 15 December 2020; Revised: 7 May 2021; Accepted: 18 June 2021

---

## Abstract

The aim of this research was to determine the optimum parameters for synthesis and characterization of mixed rare earth hydroxide (for use as a catalyst) through co-precipitation, with sodium hydroxide as precipitation agent at pH 12. The effects of precipitation temperature (30 ,60 or 100 °C) and stirring speed (400 or 600 rpm) on the chemical composition, crystal structure and surface characteristics of the catalyst were investigated. The chemical composition of the catalyst was analyzed using X-ray fluorescence (XRF), and it was composed of $CeO_2$, $Nd_2O_3$, $La_2O_3$, and $Y_2O_3$. X-ray diffraction (XRD) studies indicated that all samples had cubic structure of $CeO_2$. The optimal temperature and stirring speed for precipitation of mixed rare earth catalyst were 60 °C and 400 rpm, respectively, giving large specific surface after calcination at 300 °C. The high 190 $m^2\ g^{-1}$ BET surface area and 1220 $\mu mol\ g^{-1}$ total basic sites were achieved, indicating small crystallite sizes and large amount of active sites in the catalyst. From the above results, the optimized catalyst is considered a promising solid catalyst for biodiesel production.

**Keywords:** mixed rare earth hydroxide, co-precipitation, catalyst, characterization, biodiesel

---

## 1. Introduction

Rare earth elements (REEs) or rare-earth metals are elements within the lanthanide series, consisting of 15 elements including scandium and yttrium (Tyler, 2004). Normally, the rare earth elements are divided into two subgroups: the light rare earth elements (LREEs) or Cerium group (La, Ce, Pr, Nd and Sm); and the heavy rare earth elements (HREEs) (Eu, Gd, Tb, Dy, Ho, Er, Tm, Yb, Lu and Y). Rare earth metal oxides are common catalysts or catalyst supports. Catalysts based on metal oxide nanoparticles (NPs) have received much attention because of their excellent high catalytic activity (Navalón & García, 2016). Metal oxide nanoparticles have a high specific surface area, which can increase the catalytic activity, and they can be easily recycled.

Currently, the world's primary energy sources are fossil fuels including oil, natural gas, and coal. The widely used fossil fuels have two major issues of concern, namely being non-renewable and harmful to the environment when combusted, via greenhouse gas emissions (Abdallah & El-Shennawy, 2013; Perera, 2018). To overcome these challenges, renewable energy sources such as biofuels (especially biodiesel) are assessed in many countries. Biodiesel is a renewable fuel, environmentally friendly and biodegradable in nature (Singaram, 2009). It can satisfy energy safety requirements without compromising engine performance. Biodiesel production is mostly carried out with homogeneous catalyst base in transesterification reactions

---

♣Peer-reviewed paper selected from The 9th International Conference on Engineering and Technology (ICET-2021)

*Corresponding author
Email address: dussadeer@tint.or.th

using alkaline catalysts. However, the separation and recovery are still difficult when using a homogeneous catalytic system (Cole-Hamilton, 2003). Some studies have reported the use of heterogeneous catalysts in biodiesel production via transesterification, with improved specific catalytic activity over the homogeneous catalysts and without catalytic activity loss (Semwal, Arora, Badoni, & Tuli, 2011; Thangaraj, Solomon, Muniyandi, Ranganathan, & Lin, 2019).

Rare earths such as cerium and lanthanum have been reported as promising heterogeneous catalysts for biodiesel synthesis from vegetable oils with methanol. This is due to the presence of dual strong acidic and basic sites, as well as good stability. Zhao *et al.* (2019) have studied a metal oxide catalyst for biodiesel production by transesterification of palm oil, using lanthanum-dolomite as the heterogeneous catalyst. A high biodiesel yield of 98.7% was achieved. The dolomite when incorporated with cerium catalyst could catalyze transesterification and achieve biodiesel yield of 97.21%, according to Niu *et al.* (2020)

There have been very few studies on the synthesis and characterization of mixed rare earth catalysts for biodiesel production, especially on the catalytic activity in simultaneous esterification and transesterification. Therefore, in this work, mixed rare earth hydroxide cake obtained from monazite concentrate processing was utilized to prepare heterogeneous nanocatalysts. The effects of precipitation temperature and stirring speed on the physicochemical properties were assessed in a preliminary study. It is expected that the prepared catalysts would have high specific surface area with a large number of basic/acidic sites. The catalyst will be used to catalyze simultaneous esterification and transesterification of palm oil in the presence of oleic acid with methanol, for biodiesel production in the next experiment.

## 2. Materials and Methods

### 2.1 Catalyst preparation

The raw mixed rare earth hydroxide cake, received from monazite concentrate processing, was used to synthesize catalysts by co-precipitation method. The mixed rare earth hydroxide cake (20 g) was dissolved in 6 M HCl to a final volume of 250 ml. The solution was precipitated with NaOH (20 %wt) at 30, 60 or 100 ºC, with stirring speed of 400 or 600 rpm, until pH reached 12. The precipitate was washed with distilled water and then dried at 110 ºC for 12 h. The dried sample was calcined in a furnace at 300 °C for 3 h to obtain mixed rare earth catalysts. The prepared catalysts before and after drying are demonstrated in Figure 1. The different conditions for precipitation of mixed rare earth hydroxide catalyst are shown in Table 1.

### 2.2 Catalyst characterization

The crystal structures of catalysts were identified by using a Bruker-AXS, D8 AVANCE, X-ray diffraction spectrometer (XRD) equipped with Cu Kα radiation source (λ = 1.5406 Å). The diffraction patterns were collected at 25 °C and over an angular range from 10 to 90º with a step size of 0.039º and a step time of 1 sec. The elemental compositions of the mixed rare earth catalysts were analyzed using a Bruker S8 Tiger wavelength dispersive X-ray fluorescence (WD-XRF) device. Nitrogen adsorption-desorption isotherms were obtained at 77 K on a 3Flex Surface Characterization Analyzer (Micromeritics Instrument Corporation, Norcross, USA). Brunauer–Emmett–Teller (BET) method and Barrett-Joyner-Halenda (BJH) analysis were used to determine the surface area, particle size, and pore volume distribution of the catalysts. Temperature-programmed desorption of $CO_2$ (TPD-$CO_2$) was performed on a Micromeritics AutoChem 2910 chemisorption analyzer.

Figure 1. Mixed rare earth catalysts precipitated at pH 12 and stirring rate of 400 rpm (a) before calcination, and (b) after calcination at 300 ºC for 3 h.

Table 1. Operating conditions tested for precipitation of mixed rare earth catalysts.

| Sample | Operating conditions | |
|---|---|---|
| | Precipitation temperature (ºC) | Stirring speed (rpm) |
| Mx-1 | 30 | 400 |
| Mx-2 | 60 | |
| Mx-3 | 100 | |
| Mx-4 | 30 | 600 |
| Mx-5 | 60 | |
| Mx-6 | 100 | |

## 3. Results and Discussion

Figures 2a and 2b show the XRD patterns of mixed rare earth catalyst from the various precipitation conditions. It is observed that the peak positions of the samples are in good agreement with cubic phase of $CeO_2$ after calcination at 300 ºC. The characteristic XRD peaks are identified at 2θ = 28.5, 33.9, 47.8 and 56.2 (JCPDS file No.78-0694) corresponding to (111), (200), (220) and (311) planes, respectively. Moreover, all the XRD patterns with broad peaks indicate the formation of small-sized and poorly crystalline catalyst (Moreau *et al.*, 2013). The average crystallite size of catalyst was calculated by using the most intense peak at full width at half maximum (FWHM), based on the Debye-Scherrer formula (Patterson, 1939) as follows.

$$D = \frac{0.89\lambda}{\beta \cos\theta} \tag{1}$$

where $D$ is the crystallite size, $\lambda$ is the wavelength of X-rays, $\beta$ is the Full Width at Half Maximum (FWHM) of the Bragg diffraction peak (in radians) and $\theta$ is the diffraction angle of the reflection. The average crystallite sizes for Mx-1, Mx-2, Mx-3, Mx-4, Mx-5 and Mx- 6 catalysts were 4.07, 3.97, 3.60, 3.86, 4.12 and 3.97 nm, respectively, as shown in Table 3,

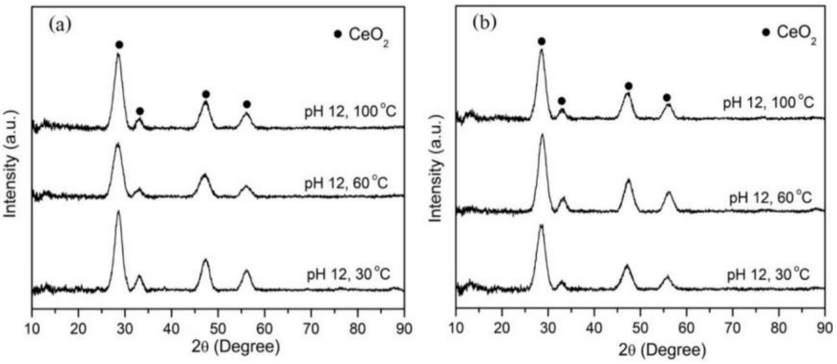

Figure 2. XRD patterns of mixed rare earth catalysts precipitated at pH 12, at stirring speed of (a) 400 rpm, and (b) 600 rpm at various precipitation temperatures.

Table 2. Chemical compositions of mixed rare earth catalysts prepared at various operating conditions as measured by XRF.

| Element | Concentration (wt%) | | | | | |
|---|---|---|---|---|---|---|
| | 30 °C | | 60 °C | | 100 °C | |
| | 400 rpm | 600 rpm | 400 rpm | 600 rpm | 400 rpm | 600 rpm |
| $CeO_2$ | 62.13 | 67.03 | 66.39 | 64.55 | 66.25 | 66.68 |
| $Nd_2O_3$ | 11.84 | 12.51 | 12.22 | 12.60 | 12.85 | 12.72 |
| $La_2O_3$ | 6.17 | 6.65 | 6.38 | 6.50 | 6.21 | 6.49 |
| $Y_2O_3$ | 3.21 | 3.35 | 3.25 | 3.36 | 3.41 | 3.32 |
| $Pr_6O_{11}$ | 2.46 | 2.69 | 2.66 | 2.71 | 2.84 | 2.72 |
| $Sm_2O_3$ | 2.35 | 2.57 | 2.54 | 2.80 | 2.83 | 2.66 |
| $Gd_2O_3$ | 1.42 | 1.76 | 1.74 | 1.74 | 1.59 | 1.71 |

indicating that the precipitation temperature and stirring speed had no significant effect on average crystallite size of catalyst.

The chemical compositions of catalyst samples measured using WDXRF are summarized in Table 2. As can be seen from the table, the precipitation temperature and stirring speed did not significantly affect chemical composition of the catalyst. However, a smaller content of individual rare earth was precipitated at 30 °C and 400 rpm stirring speed, indicating that the higher 600 rpm stirring speed was required to precipitate the rare earth elements at 30 °C. The main components of catalysts were $CeO_2$ (62-66 wt%), $Nd_2O_3$ (12-13 wt%) and $La_2O_3$ (6-7 wt%). It has been reported that three rare earth elements could efficiently catalyze both transesterification and esterification reactions to produce biodiesel (Sajith *et al.*, 2010; Vieira et.al, 2013; Li *et al.*, 2015). Other rare earth elements including $Y_2O_3$ (3 wt%), $Pr_6O_{11}$ (2-3 wt%), $Sm_2O_3$ (2-3 wt%) and $Gd_2O_3$ (1-2 wt%) were also found in the catalysts.

The effects of temperature on the precipitation were such that at a higher reaction temperature the sedimentation time of rare-earth catalysts was shorter and with higher solubility than at low temperatures (Maqbool, Srikiratiwong, & Fogler, 2011). In addition, the stirring speed also had an effect on the outcome. By stirring the slurry at a high speed, the solutions are easily mixed together. This is because of the increased suspension viscosity during precipitation, which results in shorter sedimentation time than at a low stirring speed.

The nitrogen adsorption-desorption isotherm profiles of catalysts are shown in Figure 3. All the adsorption-desorption isotherms were of Type IV. The hysteresis loops of Mx-1, Mx-3, Mx-4 and Mx-6 samples were of Type H3, while the Mx-2 and Mx-5 samples exhibited Type H4 hysteresis loops in the IUPAC classification, indicating mesoporous materials. The surface area, total pore volume and average pore diameter of catalysts are summarized in Table 3. An increase in precipitation temperature from 30 to 60 °C greatly increased specific surface from 99.67 to 190.21 $m^2 g^{-1}$ at 400 rpm stirring speed. However, a further increase of the precipitation temperature to 100 °C decreased the specific surface to 168.49 $m^2 g^{-1}$. The same trend was observed at 600 rpm stirring speed. The total pore volume showed a similar trend to surface area. The average pore diameter of catalysts was in the range of 4-7 nm. This result matches the XRD results that showed extremely high surface areas and small crystallite sizes of catalyst (Bueno-Ferrer, Parres-Esclapez, Lozano-Castelló, & Bueno-López, 2010). The total pore volume was in the range of 0.17-0.37 $cm^3 g^{-1}$. Normally, the catalytic activity of a solid catalyst in esterification and transesterification corresponds to the amount of basic/acidic sites on the catalyst; a high specific surface of the catalyst could enable a large amount of basic/acidic sites. It can be seen that the mixed rare earth oxide catalyst precipitated at 60 °C and 400 rpm exhibited high surface area, which could lead to more efficient catalytic activity in biodiesel production (Argyle & Bartholomew, 2015).

TPD profiles of $CO_2$ adsorbed on mixed rare earth catalysts, for cases with the highest and the lowest specific surface areas, are shown in Figure 4; and the basicity of the catalysts is summarized in Table 4. Three $CO_2$-TPD peaks were divided to weakly basic sites (desorption occurred in the range 100-200 °C), moderately basic sites (desorption occurred in the range 200-400 °C) and strongly basic sites (desorption occurred above 400 °C) (Madduluri *et al.*, 2020). As can be seen from Figure 4, the mixed rare earth catalysts precipitated at 30 °C showed three $CO_2$ desorption peaks, a small one at 94 °C and two broad peaks at 345 and 900 °C, attributed to the presence of weak, medium and strong basic sites, respectively. Meanwhile, a broader $CO_2$ desorption peak at 344 °C was ascribed to moderately basic sites was observed for mixed rare earth catalysts precipitated at 60 °C. There was a small desorption peak at 104°C attributed to weakly basic site. A very small peak at 893 °C was attributed to a strongly

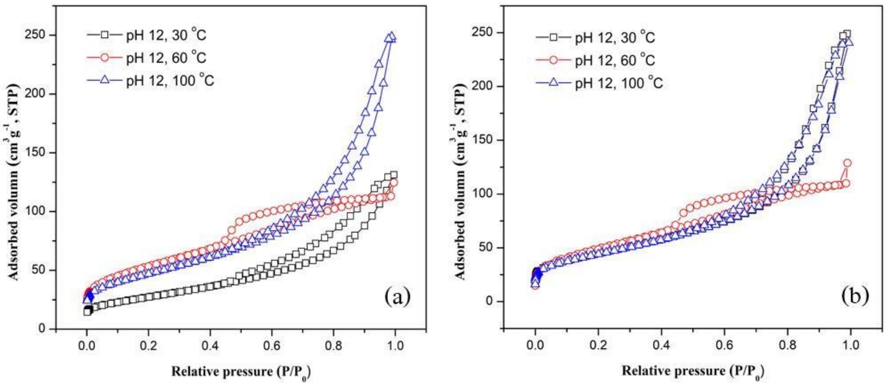

Figure 3. $N_2$ adsorption-desorption isotherms of mixed rare earth catalysts precipitated at pH 12, and stirring speed of (a) 400 rpm, and (b) 600 rpm at various precipitation temperatures.

Table 3. Physicochemical properties of mixed rare earth catalysts prepared at various operating conditions.

| Operating conditions | | Crystallite size (nm) | BET surface area ($m^2$ $g^{-1}$) | Average pore size diameter (nm) |
|---|---|---|---|---|
| Precipitation temperature (ºC) | Stirring speed (rpm) | | | |
| 30 | 400 | 4.07 | 99.67 | 7.46 |
| 60 | 400 | 3.97 | 190.21 | 4.04 |
| 100 | 400 | 3.60 | 168.49 | 9.11 |
| 30 | 600 | 3.86 | 159.65 | 9.72 |
| 60 | 600 | 4.12 | 179.05 | 4.29 |
| 100 | 600 | 3.97 | 158.08 | 9.27 |

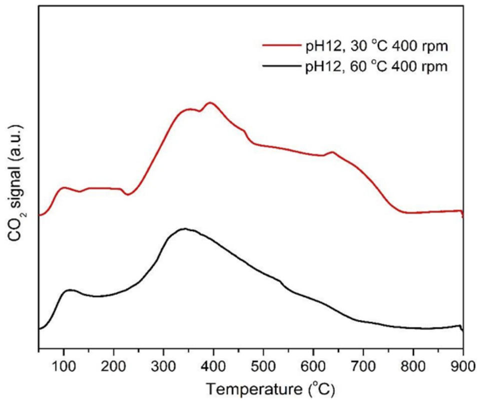

Figure 4. CO2-TPD profiles of mixed rare earth catalysts

Table 4. Basicity of mixed rare earth catalysts prepared at various operating conditions.

| Operating conditions | | Basicity (µmol/g) | | |
|---|---|---|---|---|
| Precipitation temperature (ºC) | Stirring speed (rpm) | Weak | Moderate | Strong |
| 30 | 400 | 20.43 | 373.19 | 193.47 |
| 60 | 400 | 66.72 | 1153 | 5.60 |

basic site. Table 4 shows that mixed rare earth catalysts precipitated at 30 ºC gave the most strongly basic sites with a total basicity of 587.10 µmol $g^{-1}$. Meanwhile, catalysts precipitated at 60 ºC presented the most medium basic sites with the highest total basicity of 1219.72 µmol $g^{-1}$, reflecting the high surface area of the catalyst. It can be concluded that the higher precipitation temperature could promote medium basic sites while the lower temperature offered formation of strongly basic sites. The basic site density of catalyst promotes adsorption for catalytic reaction of reactants, improving the yield in biodiesel production (Pan, Peng, Sun, Wang, & Wang, 2014). In further studies, two synthesized catalysts will be tested for catalytic activity in simultaneous transesterification and esterification of palm oil with methanol.

## 4. Conclusions

Mixed rare earth catalysts were synthesized by co-precipitation at a constant pH of 12. The influence of precipitation temperature (30, 60 or 100 ºC) and stirring speed (400 or 600 rpm) on the physiochemical properties of catalyst were investigated. The XRD results showed cubic phase of $CeO_2$ as the dominant phase with crystallite size range of 3-4 nm. The XRF analysis confirmed that $CeO_2$, $Nd_2O_3$ and $La_2O_3$ were predominantly present in the catalysts. The highest BET surface area of mixed rare-earth oxide catalysts of 190 $m^2$ $g^{-1}$ was achieved under the following conditions: precipitation temperature 60 ºC and stirring rate 400 rpm. These gave the largest amount of basic sites, at 1219.72 µmol $g^{-1}$. At the lower precipitation temperature of 30 ºC, strongly basic sites were formed on the catalyst. It could be expected that the catalyst with high surface area and large number of basic sites would provide good catalytic activity in biodiesel reaction.

The synthesized catalysts will be further investigated for their catalytic activities in simultaneous transesterification and esterification reactions for biodiesel production. In addition, the effects of precipitation pH on the chemical composition and physicochemical properties of catalyst will be assessed.

## References

Abdallah, L. & El-Shennawy, T. (2013). Reducing carbon dioxide emissions from electricity sector using smart electric grid applications. *Journal of Engineering*, *2013*. doi:10.1155/2013/845051

Argyle M. D., & Bartholomew, C. H. (2015). Heterogeneous catalyst deactivation and regeneration: a review. *Catalysts*, *5(*1), 145-269. doi:10.3390/catal5010145

Bueno-Ferrer, C., Parres-Esclapez, S., Lozano-Castelló, D., & Bueno-López, A. (2010). Relationship between surface area and crystal size of pure and doped cerium oxides. *Journal of Rare Earths*, *28*(5), 647-653. doi:10.1016/S1002-0721(09)60172-1

Cole-Hamilton, D. J. (2003). Homogeneous catalysis--new approaches to catalyst separation, recovery, and recycling. *Science*, *299*(5613), 1702-1706. doi:10. 1126/science.1081881

Li, X., Tong, D., & Hu, C. (2015). Efficient production of biodiesel from both esterification and transesterification over supported $SO_4^{2}$–$MoO^{3-}$–$ZrO_2$– $Nd_2O_3/SiO_2$ catalysts. *Journal of Energy Chemistry*, *24*(4), 463-471.

Madduluri, V. R., Nagaiah, P., Prathap, C., Vasikerappa, K., Nagu, A., Raju, B. D., & Rao, K. S. R. (2020). Synergistic interface between $Co_3O_4$ and $MgAl_2O_4$ in $CO_2$ assisted continuous vapor phase oxidative dehydrogenation of ethylbenzene to styrene monomer. *Arabian Journal of Chemistry*, *13*(1), 2883- 2896.

Maqbool, T., Srikiratiwong, P., & Fogler, H. S. (2011). Effect of temperature on the precipitation kinetics of asphaltenes. *Energy and Fuels*, *25*(2), 694-700. doi:10.1021/ef101112r

Moreau, L. M., Ha, D. H., Zhang, H., Hovden, R., Muller, D. A., & Robinson, R. D. (2013). Defining crystalline/ amorphous phases of nanoparticles through X-ray absorption spectroscopy and X-ray diffraction: The case of nickel phosphide. *Chemistry of Materials*, *25*(12), 2394-2403. doi:10.1021/cm303490y

Navalón, S. & García, H. (2016). Nanoparticles for Catalysis. *Nanomaterials*, *6*(7), 123. doi:10.3390/nano60701 23.

Niu, S., Zhang, X., Ning, Y., Zhang, Y., Qu, T., Hu, X., . . . Lu, C. (2020). Dolomite incorporated with cerium to enhance the stability in catalyzing transesterification for biodiesel production. *Renewable Energy*, *154*, 107-116 doi:10.1016/j.renene.2020.03.003

Pan, Q., Peng, J., Sun, T., Wang, S., & Wang, S. (2014). Insight into the reaction route of $CO_2$ methanation: Promotion effect of medium basic sites. *Catalysis Communications*, *45*, 74-78.

Patterson, A. L. (1939). The Scherrer formula for X-ray particle size determination. *Physical Review*, *56*(10), 978.

Perera, F. (2018). Pollution from fossil-fuel combustion is the leading environmental threat to global pediatric health and equity: solutions exist. *International Journal of Environmental Research and Public Health*, *15*(1), 16. doi:10.3390/ijerph15010016

Sajith, V., Sobhan, C. B., & Peterson, G. P. (2010). Experimental investigations on the effects of cerium oxide nanoparticle fuel additives on biodiesel. *Advances in Mechanical Engineering*, *2*, 581407.

Semwal, S., Arora, A. K., Badoni, R. P., & Tuli, D. K. (2011). Biodiesel production using heterogeneous catalysts. *Bioresource Technology*, *102*(3), 2151-2161. doi:10. 1016/j.biortech.2010.10.080

Singaram, L. (2009). Biodiesel: An eco-friendly alternate fuel for the future: A review. *Thermal Science*, *13*(3), 185-199. doi:10.2298/TSCI0903185S

Thangaraj, B., Solomon, P. R., Muniyandi, B., Ranganathan, S., & Lin, L. (2019). Catalysis in biodiesel production-a review. *Clean Energy*, *3*(1), 2-23. doi:10.1093/ce/zky020

Tyler, G. (2004). Rare earth elements in soil and plant systems-A review. *Plant and Soil*, *267*(1-2), 191-206. doi:10.1007/s11104-005-4888-2.

Vieira, S. S., Magriotis, Z. M., Santos, N. A., Saczk, A. A., Hori, C. E., & Arroyo, P. A. (2013). Biodiesel production by free fatty acid esterification using lanthanum ($La^{3+}$) and HZSM-5 based catalysts. *Bioresource Technology*, *133*, 248-255.

Zhao, S., Niu, S., Yu, H., Ning, Y., Zhang, X., Li, X., Zhang, Y., Lu, C., & Han, K. (2019). Experimental investigation on biodiesel production through transesterification promoted by the La-dolomite catalyst. *Fuel*, *257*, 116092. doi:10.1016/j.fuel.2019. 116092